

DMH-HARQ: Reliable and Open Latency-Constrained Wireless Transport Network

Bin Han, *Senior Member, IEEE*, Muxia Sun, *Member, IEEE*, Yao Zhu, *Member, IEEE*,

Vincenzo Sciancalepore, *Senior Member, IEEE*, Mohammad Asif Habibi, Yulin Hu, *Senior Member, IEEE*, Anke Schmeink, *Senior Member, IEEE*, Yanfu Li, *Senior Member, IEEE*, Hans D. Schotten, *Member, IEEE*

The extreme requirements for high reliability and low latency in the upcoming Sixth Generation (6G) wireless networks are challenging the design of multi-hop wireless transport networks. Inspired by the advent of the virtualization concept in the wireless networks design and *openness* paradigm as fostered by the Open-Radio Access Network (O-RAN) Alliance, we target a revolutionary resource allocation scheme to improve the overall transmission efficiency.

In this paper, we investigate the problem of automatic repeat request (ARQ) in multi-hop decode-and-forward (DF) relaying in the finite blocklength (FBL) regime, and propose a dynamic scheme of multi-hop hybrid ARQ (HARQ), which maximizes the end-to-end (E2E) communication reliability in the wireless transport network. We also propose an integer dynamic programming (DP) algorithm to efficiently solve the optimal Dynamic Multi-Hop HARQ (DMH-HARQ) strategy. Constrained within a certain time frame to accomplish E2E transmission, our proposed approach is proven to outperform the conventional listening-based cooperative ARQ, as well as any static HARQ strategy, regarding the E2E reliability. It is applicable without dependence on special delay constraint, and is particularly competitive for long-distance transport network with many hops.

Index Terms—6G, URLLC, HARQ, openness, relay, FBL, dynamic programming

I. INTRODUCTION

Ultra-reliable low-latency communications (URLLC) is pushing wireless transport beyond fiber-based backhaul toward multi-hop wireless chains that stitch together terrestrial small cells and non-terrestrial segments within virtualized, Open-Radio Access Network (O-RAN) [6]–[8]. In such deployments, fronthaul, midhaul, and backhaul flows may traverse sequences of open radio hardware unit (O-RU), open distributed unit (O-DU), and open centralized unit (O-CU) nodes hosted on O-Cloud and orchestrated by the SMO, with the specific chain length and composition dictated by functional splits and dynamic placement.

The shift to millimeter-wave (mmWave) and (sub-)THz for capacity and positioning tightens line-of-sight constraints and shrinks cell footprints, making dense, relay-rich topologies economically preferable to ubiquitous fiber [9], [10]. At the same time, 3D coverage objectives fold in non-terrestrial network (NTN) elements—unmanned aerial vehicles (UAVs),

high altitude platforms (HAPs), and satellites—whose heterogeneous channels and feedback latencies further complicate transport [11]. While relays have long been used to extend coverage and combat fading [1], [2], URLLC alters the operating point: packets are short (finite blocklength), feedback and control overheads are non-negligible, and strict end-to-end (E2E) deadlines mean that each retransmission on one hop directly consumes the time/frequency budget of successor hops. Under these conditions, classical relaying and ARQ/hybrid ARQ (HARQ) designs (tuned for long codes and per-hop optimization) systematically misestimate reliability and cannot coordinate retransmissions and forwarding at the granularity and speed demanded by URLLC [4], [5].

Challenges. The first challenge is reliability composition under finite blocklength (FBL): with short codes, per-hop decoding errors remain non-negligible and compound across hops, making E2E reliability exquisitely sensitive to how retransmissions and forwarding are budgeted within a tight delay. Second, resources are coupled across hops; allocating more symbols to a retransmission on one hop reduces the symbols—and thus reliability—available to successor hops. Third, links at mmWave and (sub-)THz under strict power limits and interference are brittle, while NTN segments (UAVs, HAPs, satellites) introduce heterogeneous channels and feedback delays. Fourth, open and disaggregated O-RAN deployments with flexible functional splits (O-RU/O-DU/O-CU, O-Cloud, SMO) yield relay chains whose length and per-hop characteristics vary with placement and load, challenging fixed frame designs and static schedulers.

Limitations of existing methods. Classical relaying assumes long codes and asymptotic coding gains, which do not hold in the FBL regime of short packets [4], [5]. Standard ARQ/HARQ mechanisms are tuned to per-hop reliability or subframe-level allocation and do not perform outcome-conditioned reallocation under a global E2E deadline, thereby neglecting the inter-hop coupling central to URLLC. Fixed retransmission counts, timers, or frame partitions cannot adapt to instantaneous decode outcomes, hop heterogeneity, or O-RAN-driven topology changes. Even listening-based cooperative automatic repeat request (ARQ) [12] typically moves resources at the frame/subframe timescale: when packets are short, symbol-level decisions become pivotal yet are unsupported.

Contributions. We propose a dynamic HARQ scheme for multi-hop relaying in the FBL regime that reallocates—at *channel-use (symbol) granularity*—the remaining radio budget between the current hop’s repeats and successor hops, conditioned on instantaneous decode outcomes. The design

B. Han, M. A. Habibi, and H. D. Schotten are with RPTU Kaiserslautern-Landau. M. Sun and Y.-F. Li are with Tsinghua University. Y. Zhu, Y. Hu, and A. Schmeink are with RWTH Aachen University. V. Sciancalepore is with NEC Laboratories Europe. Y. Zhu and Y. Hu are with Wuhan University. H. D. Schotten is with the German Research Center for Artificial Intelligence (DFKI). B. Han (bin.han@rptu.de) is the corresponding author.

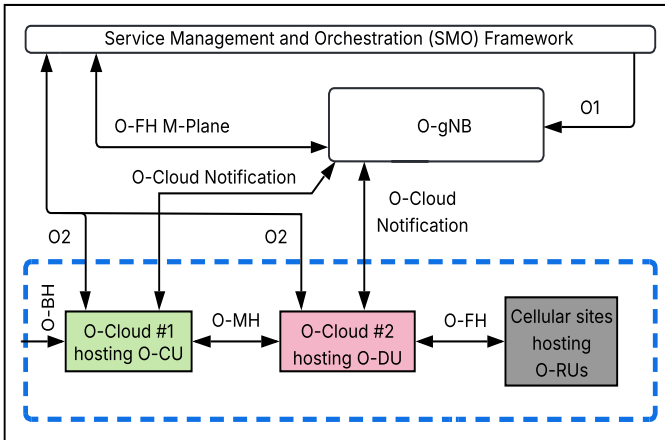


Fig. 1: A conceptual depiction of the O-RAN architecture is presented. This article concentrates on the areas outlined by the dashed blue box, where the proposed transmission scheme enhances E2E communication reliability.

is O-RAN-compatible (Fig. 1) and targets open, disaggregated transport. Our key insight is to treat retransmissions and forwarding as a single coupled E2E optimization rather than per-hop tuning, updating the residual budget after each (re)transmission using posterior success probabilities under FBL. We formalize the scheduler and provide a dynamic programming (DP) algorithm that optimizes the sequence of (re)transmissions across hops under latency and reliability targets.

In summary, our contributions are as follows: *i*) a dynamic, symbol-level HARQ framework that explicitly couples retransmission and forwarding under a strict E2E deadline, *ii*) an FBL-based analysis that quantifies reliability composition across hops, and *iii*) a DP-based optimal scheduler with implementable policies aligned with O-RAN disaggregation. Compared to static HARQ, subframe-level listening-based cooperative ARQ [12], and long-code-inspired relaying [1], [2], our approach delivers improved reliability–latency trade-offs for URLLC over O-RAN-inspired wireless transport.

The remainder of the paper is organized as follows: We begin with Section II to provide a brief review to selected literature in related field. Section III follows to describe and formulate the investigated problem, which is then analyzed in Section IV and solved in Section V. The proposed methods are numerically evaluated in Section VI, followed by some further discussions in Section VII. To the end, we close the paper with our conclusion and outlooks in Section VIII.

II. RELATED WORK

The problem of multi-hop relay has been attracting great interest in the wireless field since long, for it has a rich potential to offer extended cell coverage and improved channel capacity [1], particularly in the O-RAN architecture [15], [16]. Generally, there are two families of relay technologies, namely decode-and-forward (DF) and amplify-and-forward (AF). Albeit the disadvantage of higher implementation complexity, DF comprehensively outperforms AF in latency-reliability performance [17], and is therefore preferred by

many researchers. Literature has investigated multi-hop DF from various perspectives, including modulation scheme [18], selective relaying route [19], and relay station placement [20], and ARQ strategy [21].

Over the past few years, the emerging wireless use scenario of URLLC in O-RAN is challenging off-the-shelf multi-hop relay. The extreme requirement of low end-to-end (E2E) latency in O-RAN URLLC is leading to even more stringent time constraint over each individual hop [22], [23], which is barely achievable with conventional technologies. To meet such a stringent latency requirement, URLLC transmissions are likely carried out with short packet, i.e., the codewords cannot be considered as infinite long. With such so-called FBL codes, many theories and propositions in classical information theory fail to apply since the Shannon limit is no more asymptotically achievable. To accurately characterize the relationship between achievable data rate and reliability in the FBL regime, *Polyanskiy et al.* derived in [24] a closed-form expression for the single-hop transmission in additive white Gaussian noise (AWGN) channels. Later on, this FBL characterization was generalized, extended into Gilbert-Elliott channels [25] and quasi-static flat-fading channels [26]. Recently, the FBL model in random access channel has also been analyzed [27]. On the basis of those results, the performance FBL communication systems has been investigated in context of various wireless networking technologies, such as multi-input multi-output (MIMO) [28], orthogonal frequency-division multiple access (OFDMA) [29], non-orthogonal multiple access (NOMA) [30] and multi-access edge computing (MEC) [31].

Specifically for FBL relay networks, the system performance are generally investigated in a deterministic manner in the most existing works [4], [32]–[35]. In particular, the authors of [4] studied the performance bound of two-hop FBL relay system with perfect channel state information (CSI), which was later extended to the scenarios with only partial CSI available [32]. Moreover, the authors of [33] investigated a potential use case where UAV behaves as the relay between source and destination to improve the system performance. Energy harvesting was introduced in [34] where the relay solely relies on the harvested energy to forward the information. The authors of [35] studied the impact of imperfect successive interference cancellation (SIC) in NOMA schemes on relay system that causes by the FBL transmission error.

Another interesting FBL use case is the closed-loop communication, which is not only common in MEC scenarios but also strongly related to FBL relay networks, because it behaves in a similar way as a two-hop relay chain does. In a previous work of ours we proposed for this use case the so-called Closed-Loop ARQ (CLARQ) algorithm [36], which dynamically re-allocates blocklengths between uplink retransmission and downlink reception, so as to minimize the closed-loop error rate. Moreover, in [37] we analyzed the optimal one-shot transmission scheme, which is a special case of CLARQ, under both constraints of latency and energy consumption.

III. PROBLEM SETUP

In context of the O-RAN architecture [8], we consider a multi-hop data link in the wireless transport network, which has three stages: the O-RU is connected to the O-DU over a wireless fronthaul, the O-DU to the O-CU over a wireless midhaul, and the O-CU to the core network over a wireless backhaul. Upon the specific function splitting and orchestration scheme, a VNF may be flexibly placed at the O-RU, O-DU, or O-CU. In the latter two cases, data involved with the virtualized network function (VNF) must be decoded and forwarded over one or multiple hops from the O-RU to the implementation node of the VNF in the uplink (UL), or in the inverse direction for the downlink (DL), or both for a closed-loop data link. While the wireless fronthaul has usually only one hop, both the midhaul and backhaul links can often have multiple hops, due to the high communication distance (typically between 20 km to 40 km for the midhaul and 20 km to 300 km for the backhaul [38]). Thus, the wireless transport network can be modeled as a multi-hop DF relaying chain, which is supposed to meet a stringent latency constraint.

A. Multi-Hop DF and DMH-HARQ

Now consider a multi-hop relaying chain with $I + 1$ nodes over I hops, each applying the DF strategy based on simple HARQ without combining. We assume that all channels of the I hops are i.i.d., undergoing Gaussian noise and Rician fading. We assume that every decoding process, together with the associated feedback of acknowledgement (ACK) or negative acknowledgement (NACK) to the predecessor node for the HARQ procedure, makes the same delay of T_1 . The overall transmission to a maximal E2E delay is limited to T_{\max} . For simplification of the analysis, we consider for every node the same symbol rate f_s , modulation order Q_m (and therefore the bit-time length $T_b = \frac{1}{Q_m f_s}$), transmission power P , and noise power N . The transmitting node of each hop is capable of flexibly adjust its channel coding rate in every (re-)transmission attempt independently from others. We consider in this study a block fading scenario, where the channel h_i of each hop $i \in \mathcal{I} = \{1, 2, \dots, I\}$ remains consistent over the entire time frame of T_{\max} . Each transmitting node of hop i possesses the perfect CSI of h_i , while knowing only its position in the relaying chain and the statistical CSI of all other hops.

Here we consider a problem of dynamic radio resource allocation among different HARQ slots over the I -hop DF chain. On every hop, the transmitting node can individually adjust its coding rate for the next (re)transmission. Since the modulation order and symbol rate are fixed, this will determine the time span of the transmission slot, which cannot exceed the remaining time of the entire transmission frame. If the message is successfully decoded, the successor node will take the turn and further forward the message, unless it is the sink node, i.e. the $(I+1)^{\text{th}}$. If the decoding fails, the receiving node will trigger the HARQ procedure by sending back a NACK to the transmitting node, which then keeps re-transmitting the message until either a successful reception or a timeout, i.e. when the remaining time falls insufficient to support any

further effective transmission. In every individual repeat, the node is able to readjust its coding rate. We consider a timer embedded in the header of every message, so that every node is aware of the time remaining from the T_{\max} frame. We name this proposed approach as Dynamic Multi-Hop HARQ (DMH-HARQ), which is briefly illustrated in Fig. 2 in context of an example 4-hop DF chain.

B. Binary Schedule Tree

From Fig. 2 we see that the complete schedule of DMH-HARQ has a structure of complete binary tree \mathfrak{T} , which can be recursively defined as a 3-tuple $\mathfrak{T} = (L(\mathfrak{T}), S(\mathfrak{T}), R(\mathfrak{T}))$, where $S(\mathfrak{T})$ is a singleton set containing the root node of \mathfrak{T} , $L(\mathfrak{T})$ and $R(\mathfrak{T})$ are the binary trees rooted on the left and right children of the root node, respectively:

$$L(\mathfrak{T}) = \begin{cases} \emptyset & S(\mathfrak{T}) = \emptyset, \\ (L(L(\mathfrak{T})), S(L(\mathfrak{T})), R(L(\mathfrak{T}))) & \text{o.w.,} \end{cases} \quad (1)$$

$$R(\mathfrak{T}) = \begin{cases} \emptyset & S(\mathfrak{T}) = \emptyset, \\ (L(R(\mathfrak{T})), S(R(\mathfrak{T})), R(R(\mathfrak{T}))) & \text{o.w.} \end{cases} \quad (2)$$

Each node s in the tree representing a certain system state, which can be defined as a 4-tuple $s = (t_s, i_s, k_s, \tau_s)$ where $t_s \in \mathbb{R}^+$ is the remaining time, $i_s \in \mathbb{N}$ is the remaining hops to transmit the message, $k_s \in \mathbb{N}$ is the number of failed HARQ attempts on the current hop, and τ_s the accumulated time spent on these k_s unsuccessful transmissions (excluding the feedback losses). This system state concerns various aspects of the relaying session, involving the remaining resource, the transmissions to accomplish, and partial history of previous transmissions. Take the example in Fig. 2, starting with the initial state $s_0 = (T_{\max}, 4, 0, 0)$, where the schedule assigns n_{s_0} bits for the first transmission, reserving therewith $r_{s_0} = T_{\max} - n_{s_0}T_b - T_1$ for future (re)transmissions. Upon the first transmission result, two possible succeeding states can be $s_1 = (r_{s_0}, 4, 1, n_{s_0}T_b)$ and $s_2 = (r_{s_0}, 3, 0, 0)$, respectively. Now let $n_s \triangleq n(t_s, i_s, k_s, \tau_s) \in \mathbb{N}$ denote the blocklength to be allocated at state s , according to the policy $n(\cdot)$, to the current HARQ attempt on the current hop, i.e. the $(k_s + 1)^{\text{th}}$ HARQ attempt on the $(I - i_s + 1)^{\text{th}}$ hop, when there is t_s time remaining. Thus, let \mathfrak{S} denote a schedule tree with $S(\mathfrak{S}) = \{s\}$ and \mathcal{S} the space of all feasible states, for all $s \in \mathcal{S}$, on the one hand we have for the left branch

$$S(L(\mathfrak{S}_s)) = \begin{cases} \emptyset & t_s < T_{\min}^{(i_s)}, \\ \emptyset & i_s = 0, \\ \{(t_s - n_s T_b - T_1, i_s, k_s + 1, \tau_s + n_s T_b)\} & \text{o.w.} \end{cases} \quad (3)$$

Here, $T_{\min}^{(i)} = \sum_{j=1}^i (n_{\min,j} T_b + T_1)$ where $n_{\min,j}$ is the minimal blocklength of codeword on the j^{th} last hop (which is a function of the signal-to-noise ratio (SNR) γ_i over the j^{th} last hop). Therefore, in the first case of Eq. (3), $t_s < T_{\min}^{(i_s)}$ denotes the condition that a remaining time t_s is insufficient to forward the message over the last i hops even when no

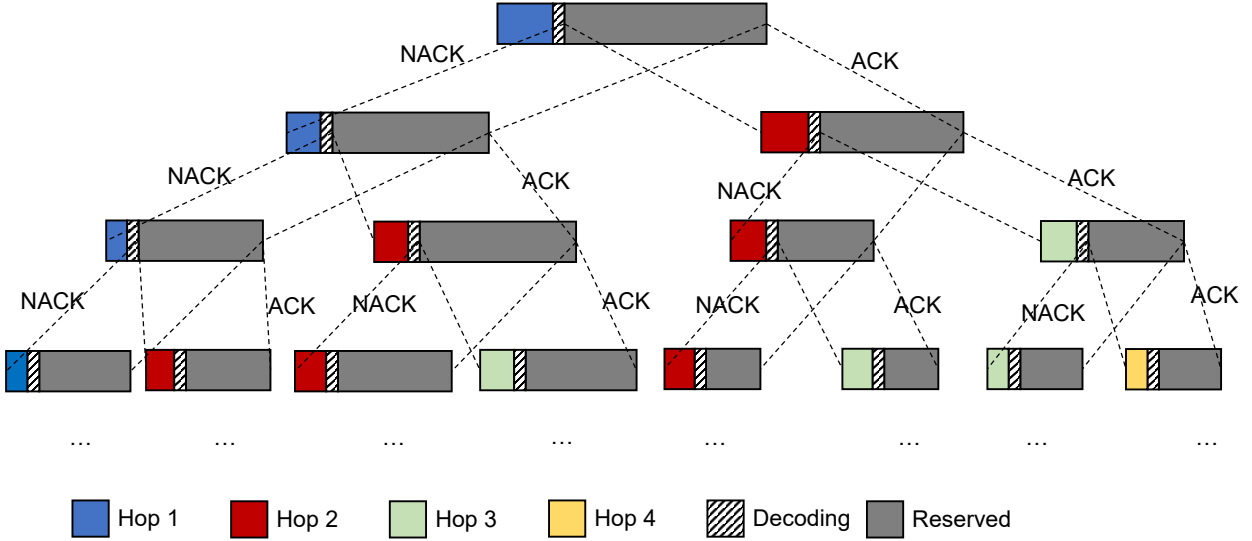


Fig. 2: Part of a DMH-HARQ schedule for 4-hop DF chain, beginning with the initial state $s_0 = (T_{\max}, 4, 0, 0)$. At each (re)transmission attempt, an optimal blocklength is calculated for consumption, and a fixed time for decoding and feedback is required. Upon the decoding result, the remaining (reserved) blocklength is dynamically assigned regarding the decoding result: either for next hops upon success (ACK), or for retransmission on the same hop upon failure (NACK). The states s_0 , s_1 , and s_2 are illustrated with time frame details.

error occurs (i.e. with only one transmission attempt on each hop), under which the DMH-HARQ procedure is terminated without success. The second case a successful completion of the DMH-HARQ over the entire chain (as there is $i = 0$ hop remaining); the third case stands for the consequence when the current HARQ attempt fails with sufficient remaining time, i.e. the message is re-transmitted over the current hop for the $(k_s + 1)^{\text{th}}$ time.

On the other hand, for the right branch we have

$$S(R(\mathfrak{T}_s)) = \begin{cases} \emptyset & t_s < T_{\min}^{(i_s)}, \\ \emptyset & i_s = 0, \\ \{(t_s - n_s T_b - T_1, i_s - 1, 0, 0)\} & \text{o.w.} \end{cases} \quad (4)$$

Again, the first case implies to insufficient remaining time and the second case describes a successful completion of DMH-HARQ. The third case stands for a successful DF over an intermediate hop, when the DMH-HARQ progresses to the next hop, i.e. the $(i_s - 1)^{\text{th}}$ last hop.

C. Optimization Problem

To measure the effectiveness of a DMH-HARQ schedule, we define a utility $\xi(\mathfrak{T}_s)$ as the chance of successfully forwarding the message over the next i_s hops within a time limit of t_s , then from the recursive structure (1)–(2) of \mathfrak{T}_s , we have

$$\xi(\mathfrak{T}_s) = \begin{cases} 0 & \mathfrak{T}_s = \emptyset, \\ 1 & i_s = 0, \\ \varepsilon_s \xi(L(\mathfrak{T}_s)) + (1 - \varepsilon_s) \xi(R(\mathfrak{T}_s)) & \text{o.w.,} \end{cases} \quad (5)$$

where ε_s is the packet error rate (PER) of the $(k_s + 1)^{\text{th}}$ HARQ attempt on the i_s^{th} last hop with codeword blocklength n_s . Since $\varepsilon_s \in [0, 1]$, we know that $\xi(\mathfrak{T}_s)$ is bounded between $[0, 1]$ for any \mathfrak{T}_s .

Thus, given the time frame length T_{\max} and total number of hops I specified, the reliability of DMH-HARQ can be optimized regarding the blocklength allocation policy n :

$$\text{maximize}_{n: \mathcal{S} \rightarrow \mathbb{N}^+} \xi(\mathfrak{T}_{s_0}) \quad (6a)$$

$$\text{subject to } n_{\min, i_s} \leq n_s \leq \frac{t_s - T_{\min}^{(i_s-1)}}{M f_s} \quad \forall s \in \mathcal{S} \quad (6b)$$

where $s_0 = (T_{\max}, I, 0, 0)$, and the action $n_s = n(s)$ is the blocklength to be allocated for the next (re)transmission at state s . The minimal blocklength n_{\min, i_s} is set here concerning the rapid decay of link reliability regarding reducing blocklength in the FBL regime. Commonly, people set an artificial constraint that the PER ε_s for any $s \in \mathcal{S}$ shall not exceed a pre-defined threshold ε_{\max} , so that

$$n_{\min, i_s} = \min\{n \in \mathbb{N}^+ \mid \varepsilon_s \leq \varepsilon_{\max}\} \quad (7)$$

It shall be noted that (6) is *not* a convex optimization problem since it is an integer programming problem. The existence (but not uniqueness) of optimal solution is guaranteed by the facts that *i*) it is a finite combinatorial optimization problem, and *ii*) the objective function is limited within the range $[0, 1]$. In the worst-efficient approach, the optimal solution can be found by exhaustive search with an exponential time complexity. For a better efficiency, as we will show in Sec. V, it can be solved within pseudo-polynomial time by means of integer dynamic programming (DP). Nevertheless, before starting with the integer DP algorithm, some analyses to a relaxed convex version of Problem (6) can provide us useful insights to the structure of the optimal solution, which are usually crucial to the design of the integer DP algorithm by means of reducing the state and action spaces to search. Such analyses will be provided in the next section.

IV. ANALYSES: TYPE I HARQ WITHOUT COMBINING

Before diving deep into the optimal HARQ scheduling problem, we shall study the error model of each HARQ attempt. For a delay-critical scenario with stringent E2E latency constraint, such as URLLC, we consider the use of short code, where the blocklength of every codeword is limited. Therefore, the PER of every HARQ attempt shall be analyzed w.r.t. the finite blocklength information theory, and the performance highly depends on the selected coding and HARQ schemes.

The choice of combining technique can have crucial impact in the performance of HARQ protocols. It is well known that among the different types of HARQ, Type I HARQ without combining provides the worst error performance with the simplest implementation, while the Type II HARQ-incremental redundancy (IR) offers the best error performance with the highest implementation complexity. On the one hand, applying Type II HARQ-IR to our DMH-HARQ protocol will certainly grant it an optimal performance. Unfortunately, however, the generic error model will therewith become analytically intractable, due to the dual inconsistencies – regarding both the redundancy rate and the frame length – over individual transmission attempts. While numerical simulations can be conducted to obtain the empirical model dedicated to any certain channel coding scheme, such models lack generality and therefore have limited theoretic contribution. On the other hand, the Type I HARQ without combining, known as the worst scheme regarding error performance, has a rich value in analysis since it outlines a tight upper-bound for PER of all HARQ solutions. Therefore, in this study we focus on the case of Type I HARQ without combining, where the receiver does not exploit any information of the unsuccessfully decoded packets.

A. Error Model, Constraints, and Approximations

Regarding Type I HARQ without combining, according to [24], the PER of an arbitrary HARQ attempt with payload length d and blocklength m on the i^{th} hop is

$$\epsilon_i(m) = Q \left(\sqrt{\frac{m}{V_i}} \left(\mathcal{C}_i - \frac{d}{m} \right) \ln 2 \right), \quad (8)$$

where for AWGN channels $V_i = 1 - \frac{1}{(1+\gamma_i)^2}$, with $\gamma_i = \frac{P g_i}{N} = \frac{P \bar{g}}{N L_{f,i}}$ denoting the SNR on the i^{th} hop. Here, g_i is the channel gain of the i^{th} hop, which is determined by the mean channel gain \bar{g} and the random fading loss $L_{f,i}$. Thus, for all $s = (t_s, i_s, k_s, \tau_s) \in \mathcal{S}$, with the blocklength allocation policy n_s , we have

$$\epsilon_s = \epsilon_{I+1-i_s}(n_s) = Q \left(\sqrt{\frac{n_s}{V_{I+1-i_s}}} \left(\mathcal{C}_{I+1-i_s} - \frac{d}{n_s} \right) \ln 2 \right), \quad (9)$$

which has no dependency on t_s , k_s or τ_s except for the potential dependency of n_s on them.

Following the common routine in FBL study, we can extend the space of blocklength from integer to real numbers, so as to allow non-integer values of n_s for the convenience of analysis (approximate integer solutions can be then obtained by

rounding the real-valued optima). Thus, the original problem (6a) can be replaced by

$$\begin{aligned} & \text{maximize} && \xi(\mathfrak{T}_{s_0}) \\ & n : \mathcal{S} \rightarrow \mathbb{R}^+ \end{aligned} \quad (10)$$

Recalling (7), the lower-bound n_{\min, i_s} in constraint (6b) can be obtained from:

$$Q \left(\sqrt{\frac{n_{\min, i_s}}{V_{I+1-i_s}}} \left(\mathcal{C}_{I+1-i_s} - \frac{d}{n_{\min, i_s}} \right) \ln 2 \right) = \epsilon_{\max}, \quad (11)$$

which depends on s only regarding i_s . Meanwhile, the upper-bound $n_{\max, s} \triangleq \frac{t_s - T_{\min}^{(i_s-1)}}{M f_s}$ is determined by both t_s and all $n_{\min, j}$ that $1 \leq j \leq i_s - 1$, i.e., by t_s and i_s .

B. Multi-Hop Link Reliability with Perfect Global CSI

Based on the error model above, we start our analysis to the optimization problem (6) with a simplified case where perfect CSI of all hops $i \in \mathcal{I}$ is available at every node. For the convenience of notation, in the analyses below we let

$$\xi_{\max}(s) \triangleq \max_{n: \mathcal{S} \rightarrow \mathbb{R}^+} \xi(\mathfrak{T}_s), \quad \forall s \in \mathcal{S}, \quad (12)$$

and the corresponding optimal blocklength allocation policy

$$n_{\text{opt}}(s) \triangleq \arg \max_{n: \mathcal{S} \rightarrow \mathbb{R}^+} \xi(\mathfrak{T}_s), \quad \forall s \in \mathcal{S}. \quad (13)$$

First, recall the remarks we made earlier in Section IV-A, that given a certain s , both the PER ϵ_s and the constraints to n_s are independent from k_s or τ_s , but determined by t_s and i_s . Thus, we can assert that

Lemma 1. *With Type I HARQ without combining, $n_{\text{opt}}(s)$ is independent from k_s or τ_s , but determined by t_s and i_s , i.e. $n_{\text{opt}}(s) = n_{i_s}^{\text{opt}}(t_s)$.*

The proof of Lemma 1 is trivial and therefore omitted.

For convenience we let $s_l(\mathfrak{T}_s)$ denote the root state of $L(\mathfrak{T}_s)$, and similarly $s_r(\mathfrak{T}_s)$ the root state of $R(\mathfrak{T}_s)$. Thus, from the recursive structure Eq. (5) of the utility $\xi(\mathfrak{T}_s)$, for all s that $\mathfrak{T}_s \neq \emptyset$ and $i_s \neq 0$, we can derive

$$\begin{aligned} & \xi_{\max}(s) \\ &= \max_{n_s} \{ \epsilon_s \xi_{\max}(s_l(\mathfrak{T}_s)) + (1 - \epsilon_s) \xi_{\max}(s_r(\mathfrak{T}_s)) \} \\ &= \max_{n_s} \left\{ \epsilon_s \max_{n_{S(L(\mathfrak{T}_s))}} \xi(L(\mathfrak{T}_s)) + (1 - \epsilon_s) \max_{n_{S(R(\mathfrak{T}_s))}} \xi(R(\mathfrak{T}_s)) \right\} \\ &= \dots \end{aligned} \quad (14)$$

which forms a Bellman equation. Under the error model (9), we have the following conclusions:

Lemma 2. *With Type I HARQ without combining, for all $s \in \mathcal{S}$ that $i_s = 1$ (i.e. on the last hop), the optimal blocklength allocation is always a one-shot transmission $n_{\text{opt}}(s) = \frac{t_s - T_1}{T_b}$ that maximizes the utility to $\xi_{\max}(s) = 1 - \epsilon_I \left(\frac{t_s - T_1}{T_b} \right)$.*

Theorem 1. *As long as $t_s \geq T_{\min}^{(i_s-1)}$ and $i_s \geq 1$, $\xi_{\max}(s)$ is a continuous and strictly monotone increasing function of t_s .*

The proofs are provided in Appendices A and B, respectively.

Algorithm 1: Integer DP for DMH-HARQ schedule optimization

```

1 function OptSchedule( $s, g_{i_s}, f_G, \varepsilon_{\max}, T_b, T_1$ ):
2    $\mathcal{D}_{\text{local}} \leftarrow \text{Dict}(\{\}, \mathcal{D}_{\text{succ}} \leftarrow \text{Dict}(\{\})$  // Empty dictionaries.
3   Best!( $t_s, i_s, g_{i_s}, f_G, \varepsilon_{\max}, \mathcal{D}_{\text{local}}, \mathcal{D}_{\text{succ}}$ ) // Solve the optimal blocklength allocation policy.
4    $\mathfrak{X}_s \leftarrow \text{ScheduleTreeGen}(t_s, i_s, 0, 0, \mathcal{D}_{\text{local}}, T_b, T_1)$  // Generate the binary schedule tree.
5 return  $\mathfrak{X}_s$ 
6
7 function Best!( $t_s, i_s, g_{i_s}, f_G, \varepsilon_{\max}, \mathcal{D}_{\text{local}}, \mathcal{D}_{\text{succ}}$ ):
8    $n_{\min, i_s} \leftarrow \min\{n : \varepsilon_s(n) \leq \varepsilon_{\max}\}$  // W.r.t. Eq. (9).
9    $\bar{n}_{\min} \leftarrow \min\{n : \bar{\varepsilon}(n) \leq \varepsilon_{\max}\}$  // W.r.t. Eq. (15).
10  if  $\mathcal{D}_{\text{local}}.\text{find}(\{t_s, i_s\}) \neq \emptyset$  then
11     $[\xi_{\text{opt}}, n_{\text{opt}}] \leftarrow \mathcal{D}_{\text{local}}.\text{find}(\{t_s, i_s\})$  // Already solved, directly read from the look-up table (LUT).
12  else if  $t_s < [(i_s - 1)\bar{n}_{\min} + n_{\min, i_s}]T_b + i_s T_1$  then
13     $[\xi_{\text{opt}}, n_{\text{opt}}] \leftarrow [0, 0]$  // Insufficient radio resource left, DMH-HARQ terminated.
14     $\mathcal{D}_{\text{local}}.\text{append}(\{t_s, i_s\} \rightarrow [\xi_{\text{opt}}, n_{\text{opt}}])$  // Append the new result to LUT.
15  else if  $i_s == 1$  then
16     $[\xi_{\text{opt}}, n_{\text{opt}}] \leftarrow [\varepsilon_s(n_{\text{opt}}), \lfloor \frac{t_s - T_1}{T_b} \rfloor]$  // Last hop, one-shot as optimum.
17     $\mathcal{D}_{\text{local}}.\text{append}(\{t_s, i_s\} \rightarrow [\xi_{\text{opt}}, n_{\text{opt}}])$ 
18  else
19     $n_{\text{opt}} \leftarrow \arg \max_n \{\varepsilon_s(n) \text{Best!}(t_s - nT_b - T_1, i_s, g_{i_s}, f_G, \varepsilon_{\max}, \mathcal{D}_{\text{local}}, \mathcal{D}_{\text{succ}})$ 
20     $+ [1 - \varepsilon_s(n)] \text{BestSucc!}(t_s - nT_b - T_1, i_s - 1, f_G, \varepsilon_{\max}, \mathcal{D}_{\text{succ}})\}$ 
21     $\xi_{\text{opt}} \leftarrow \varepsilon_s(n_{\text{opt}}) \text{Best!}(t_s - n_{\text{opt}}T_b - T_1, i_s, g_{i_s}, f_G, \varepsilon_{\max}, \mathcal{D}_{\text{local}}, \mathcal{D}_{\text{succ}}) +$ 
22     $[1 - \varepsilon_s(n_{\text{opt}})] \text{BestSucc!}(t_s - n_{\text{opt}}T_b - T_1, i_s - 1, f_G, \varepsilon_{\max}, \mathcal{D}_{\text{succ}})$ 
23     $\mathcal{D}_{\text{local}}.\text{append}(\{t_s, i_s\} \rightarrow [\xi_{\text{opt}}, n_{\text{opt}}])$ 
24  end
25 return  $\xi_{\text{opt}}$ 
26
27 function BestSucc!( $t_s, i_s, f_G, \varepsilon_{\max}, \mathcal{D}$ ):
28    $\bar{n}_{\min} \leftarrow \min\{n : \bar{\varepsilon}(n) \leq \varepsilon_{\max}\}$ 
29   if  $\mathcal{D}.\text{find}(\{t_s, i_s\}) \neq \emptyset$  then
30      $[\xi_{\text{opt}}, n_{\text{opt}}] \leftarrow \mathcal{D}.\text{find}(\{t_s, i_s\})$ 
31   else if  $t < i(\bar{n}_{\min}T_b + T_1)$  then
32      $[\xi_{\text{opt}}, n_{\text{opt}}] \leftarrow [0, 0]$ 
33      $\mathcal{D}.\text{append}(\{t_s, i_s\} \rightarrow [\xi_{\text{opt}}, n_{\text{opt}}])$ 
34   else if  $i_s == 1$  then
35      $[\xi_{\text{opt}}, n_{\text{opt}}] \leftarrow [\varepsilon_s(n_{\text{opt}}), \lfloor \frac{t_s - T_1}{T_b} \rfloor]$ 
36      $\mathcal{D}.\text{append}(\{t_s, i_s\} \rightarrow [\xi_{\text{opt}}, n_{\text{opt}}])$ 
37   else
38      $n_{\text{opt}} \leftarrow \arg \max_n \{\bar{\varepsilon}(n) \text{BestSucc!}(t_s - nT_b - T_1, i_s, f_G, \varepsilon_{\max}, \mathcal{D}) +$ 
39      $[1 - \bar{\varepsilon}(n)] \text{BestSucc!}(t_s - nT_b - T_1, i_s - 1, f_G, \varepsilon_{\max}, \mathcal{D})\}$ 
40      $\xi_{\text{opt}} \leftarrow \bar{\varepsilon}(n_{\text{opt}}) \text{BestSucc!}(t_s - n_{\text{opt}}T_b - T_1, i_s, f_G, \varepsilon_{\max}, \mathcal{D}) +$ 
41      $[1 - \bar{\varepsilon}(n_{\text{opt}})] \text{BestSucc!}(t_s - n_{\text{opt}}T_b - T_1, i_s - 1, f_G, \varepsilon_{\max}, \mathcal{D})$ 
42      $\mathcal{D}.\text{append}(\{t_s, i_s\} \rightarrow [\xi_{\text{opt}}, n_{\text{opt}}])$ 
43   end
44 return  $\xi_{\text{opt}}$ 
45
46 function ScheduleTreeGen( $t_s, i_s, k_s, \tau_s, \mathcal{D}_{\text{local}}, T_b, T_1$ ):
47   if  $\mathcal{D}_{\text{local}}.\text{find}(\{t_s, i_s\}) == \emptyset$  then
48      $\mathfrak{X}_s \leftarrow \emptyset$ 
49   else
50      $(\xi, n) \leftarrow \mathcal{D}_{\text{local}}.\text{find}(\{t_s, i_s\})$ 
51      $\mathfrak{X}_s \leftarrow (\text{ScheduleTreeGen}(t_s - nT_b - T_1, i_s, k_s + 1, \tau_s + nT_b, \mathcal{D}_{\text{local}}, T_b, T_1), \{(t_s, i_s, k_s, \tau_s)\},$ 
52      $\text{ScheduleTreeGen}(t_s - nT_b - T_1, i_s - 1, 0, 0, \mathcal{D}_{\text{local}}, T_b, T_1))$ 
53   end
54 return  $\mathfrak{X}_s$ 

```

C. Multi-Hop Link Reliability with Imperfect CSI

As we have discussed in Section III, in the multi-hop relaying scenario, it shall be considered that each node i has only a perfect CSI of the i^{th} hop. For all the successor hops $\{i+1, i+2, \dots, I\}$, it possesses only the statistical CSI, i.e. the probability density function (PDF) f_{G_i} of their channel gains g_i , which can be reasonably assumed consistent and identical for every hop $i \in \mathcal{I}$, i.e. $f_{G_i} \equiv f_G$ for all $i \in \mathcal{I}$. Thus, in an arbitrary state $s \in \mathcal{S}$ where the node $I+1-i_s$ is forwarding the message, the node cannot accurately estimate $\varepsilon_{s'}$ for any state s' that $i_{s'} < i_s$ upon the blocklength allocation $n_{s'}$ anymore, but only the expectation upon the random channel gain:

$$\bar{\varepsilon}_{s'} = \int_0^{+\infty} \varepsilon_{s'} f_G(g_{i_{s'}}) dg_{i_{s'}}. \quad (15)$$

Note that for any specific $\gamma_{i_{s'}} \geq 0$, $\varepsilon_{s'}$ is convex and monotone decreasing w.r.t. $n_{s'}$. Thus, as a linear combination of various samples of $\varepsilon_{s'}$ over $\gamma_{i_{s'}} \in [0, +\infty)$, $\bar{\varepsilon}_{s'}$ is also convex and monotone decreasing w.r.t. $n_{s'}$, so that Theorem 1 remains applicable even when only statistical CSI of for all successor hops is available at each node.

V. ALGORITHM DESIGN**A. Optimal DMH-HARQ: Integer Dynamic Programming**

From Lemma 1 we know that when applying Type I HARQ without combining, the DMH-HARQ scheduling is a typical Markov decision process (MDP), where the expected utility ξ_s from any certain status s is independent from its historical states or actions, but only relying on the remaining time t_s and the blocklength allocation policy n_s . Such kind of problems can be generally solved by recursive approaches that gradually

evaluate and improve the decision policy by traversing the entire feasible region of states, typical examples are policy iteration and value iteration. However, such approaches are challenged by two issues when dealing with Eq. (14). First, (9) provides no closed-form analytical solution n_s for an arbitrary ε_s . Second, with $n_s \in \mathbb{R}^+$, both the feasible region \mathcal{S} and the set of possible actions becomes infinite, making it impossible to traverse the solution space within limited time.

Nevertheless, it shall be remarked that the real-value relaxation $n_s \in \mathbb{R}^+$ was taken, like in classical FBL works, only for the convenience of analysis. Indeed, representing the blocklength per transmission in the unit of channel use, the final solution $n_{\text{opt}}(s)$ can only take integer values from \mathbb{N}^+ . Meanwhile, to apply FBL approaches while guaranteeing to meet the stringent latency requirement, as referred earlier, n_s is strictly constrained by (6b). Thus, both the action set and the feasible region of status are usually of reasonable sizes, enabling us to apply classical integer DP techniques to directly solve the global optimum (the feasibility and optimality of this approach are discussed in [36]). A typical implementation is to recursively solve $n_{\text{opt}}(s)$ from the last hop where $i_s = 1$ on, hop-by-hop onto the first one where $i_s = I$. The recursive algorithm is essentially accompanied with LUT to store the optimal achievable utility over the solution space, as described by Algorithm 1:

- Two global dictionaries, $\mathcal{D}_{\text{local}}$ and $\mathcal{D}_{\text{succ}}$, are defined in the main optimizing function `OptSchedule` as LUTs for the solutions of local hop (based on perfect CSI) and successor hops (based on statistical CSI), respectively. Each LUT maps the state space \mathcal{S} onto \mathbb{R}^+ to record the achievable utility $\xi_{\text{max}}(s)$.
- The functions `Best!` and `BestSucc!` are implemented to recursively solve the optimal blocklength allocation policy n_s and the associated best utility $\xi_{\text{max}}(s)$ regarding perfect and imperfect CSI, respectively. Especially, `BestSucc!` is a deviated version of `Best!` that considers with the only statistical CSI for each hop, while `Best!` exploits the perfect CSI of the local hop. `BestSucc!` is called by `Best!` to estimate the achievable utility over successor hops. *The global dictionaries dictionary $\mathcal{D}_{\text{local}}$ and $\mathcal{D}_{\text{succ}}$ are therewith updated, respectively.*
- The function `ScheduleTreeGen` is implemented to recursively generate the binary schedule tree \mathcal{T} from the dictionary $\mathcal{D}_{\text{local}}$ that stores the blocklength allocation policy.

B. Hop-by-Hop CSI Update and Reschedule

Note that by running Algorithm 1 at node $i \in \mathcal{I}$, the optimal schedule \mathcal{T}_s is solved based on the perfect CSI of the i^{th} hop and statistical CSI of all hops thereafter, which shall not be adopted by any other node. Indeed, upon a successful decoding of the message received from its predecessor node, each node $i \in \mathcal{I}$ shall individually solve its own optimal schedule \mathcal{T}_s regarding the instantaneous system state s and its real-time channel measurement g_i of the i^{th} hop. The complete procedure can be briefly summarized as in Algorithm 2. Note

that the total number of hops I is not endogenous to the algorithm, but only passed to the first node to initialize the state s . This allows our approach to be flexibly applied in the practical scenarios, where the number of hops is dynamically determined by the specific service function chain and the network topology.

Algorithm 2: I -hop DMH-HARQ with CSI update

```

1 Initialization:  $[g_1, g_2, \dots, g_I], f_G, \varepsilon_{\text{max}}, T_{\text{max}}, T_b, T_1$ 
2  $s \leftarrow (T_{\text{max}}, I, 0, 0)$ 
3 for  $i = I, I-1, \dots, 1$  do
4    $\mathcal{T}_s \leftarrow \text{OptSchedule}(s, g_i, f_G, \varepsilon_{\text{max}}, T_b, T_1)$ 
5    $s' \leftarrow s$ 
6   while true do
7     (Re)-transmit regarding  $\mathcal{T}_s$ 
8     Update  $s$  regarding the transmission result
9     if  $n_s = 0$  then
10      return // Termination state
11     else if  $i_s < i_{s'}$  then
12       break // Current hop succeeded
13     end
14   end
15 end
16 return
```

C. Computational Complexity Analysis

As described above, Algorithm 1 implements a recursive DP approach to compute the integer dynamic program. The recursive algorithm considers the DMH-HARQ as an I -stage DP problem, each stage representing a hop. Meanwhile, each hop-level sub-problem that starting with state s makes also an $\mathcal{O}(n_{\text{max},s})$ -stage DP problem itself, each stage representing an available channel use in the schedule. With any limited T_{max} , maximum of level of stage is finite and upper-bounded, i.e., $I_{\text{max}} \leq \frac{T_{\text{max}}}{M f_s n_{\text{min},i_s}}$, where n_{min,i_s} is the minimum blocklength defined in (7). Therefore, the convergence of the algorithm is guaranteed.

According to the computational complexity analysis of the CLARQ algorithm [36], which has the same structure as each hop-level sub-problem, we know that the time complexity of each hop-level sub-problem is $\mathcal{O}(n_{\text{max},s})$. Since for each $s \in \mathcal{S}$ hop, $n_{\text{max},s}$ is upper-bounded by $n_{\text{MAX}} \triangleq \frac{t_s - T_{\text{min}}^{(I-1)}}{M f_s}$, the time complexity of solving the optimal DMH-HARQ at the i^{th} last node is $\mathcal{O}(n_{\text{MAX}}^i)$. Taking the hop-by-hop execution of Algorithm 2 into account, the overall time complexity of the DMH-HARQ approach over the I -hop relay chain is $\mathcal{O}\left[\sum_{i=1}^I n_{\text{MAX}}^i\right] = \mathcal{O}(n_{\text{MAX}}^I)$, which is significantly higher than to optimize the schedule of conventional static HARQ approaches, i.e. $\mathcal{O}[\log(n_{\text{MAX}})]$.

In realistic scenarios of deployment, such a time complexity can critically challenge the online computation of optimal DMH-HARQ schedule, especially due to the time-varying channel gains g_i , which leads to high delay and significant power consumption. To address this issue, it is a practical solution to implement a LUT in each node, which that contains a set of offline solved dictionaries regarding various channel conditions, i.e., the integer DP algorithm is pre-executed offline, only the LUTs must be deployed at different relaying

nodes. Since the operation of searching for a specific entry in a dictionary-based LUT has only a time complexity of $\mathcal{O}(1)$, the devices can be rapidly adapted to the appropriate specification w.r.t. the real-time channel measurement, leading to an overall time complexity as low as $\mathcal{O}(I)$ for the entire I -hop DMH-HARQ process.

VI. NUMERICAL EVALUATION

To evaluate our proposed approaches, we conducted numerical simulations to benchmark DMH-HARQ against baseline solutions with respect to different specifications of the system and the environment.

A. Baseline Methods

Three baseline methods are implemented and evaluated in our simulations:

- 1) **Naive static HARQ-IR**: where the (re)transmission times on each hop and coding rate of every individual (re)transmission are pre-scheduled. For each hop, a full IR (Type II HARQ) is applied to combine the codes sent in different transmissions. Since the performance is highly dependent on the (re)transmission times and the coding rate, here we consider the approximate bound provided by *Makki et al.* in [5], which is only achievable with ideal Gaussian codebooks allowing non-integer blocklength. Under a naive schedule, the same length of time is assigned to every hop. Recall that the performance of Type I HARQ is guaranteed outperformed by that of Type II, and that our DMH-HARQ approach is evaluated with Type I HARQ. Therefore, the benchmark is unfairly favoring the baseline over our approach.
- 2) **Optimal static HARQ-IR**: which follows the same principle of pre-scheduled retransmission as the naive static HARQ-IR. However, the sub-frame lengths allocated to different hops are jointly optimized so as to minimize the E2E packet loss rate. Again, Type II HARQ-IR is applied and the bound in [5] is considered, granting this baseline an unfair advantage in competition against our approach.
- 3) **Listening-based cooperative ARQ**: which was proposed by *Goel et al.* in [12]. More specifically, here we consider its fully-cumulative scheme which outperforms other variants. Similar to the naive static HARQ approach, every hop is assigned with the same length of sub-frame and pre-scheduled with the same number of (re)transmissions and coding rate. However, if the DF on some hop i succeeds before using up all the pre-scheduled (re)transmission slots assigned to it, the DF on hop $i + 1$ will immediately be triggered, inheriting all the remaining time resource from its predecessor hop. In our simulation, each hop is pre-scheduled with 2 (re)transmission slots, applying Type-I HARQ without combining.

The principles of both static HARQ-IR and listening-based cooperative ARQ are illustrated in Fig. 3 for comparison with Fig. 2. Note that the naive and optimal schemes of static HARQ-IR only distinguish from each other by whether the sub-frames are of of same length over all hops.

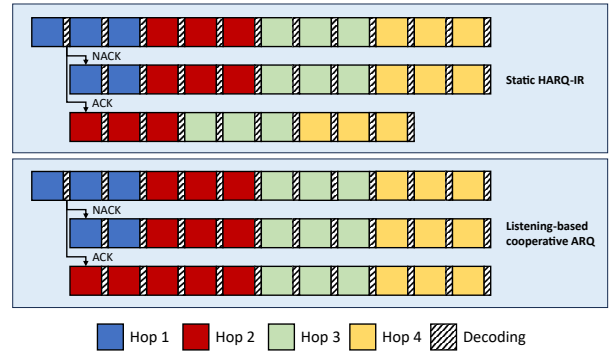


Fig. 3: Illustration of baseline solutions for 4-hop DF chain.

B. Simulation Setup

The setup of our simulation campaign is detailed in Tab. I. It is worth remarking that we consider here the E2E delay T_{\max} no longer than 1 ms. Considering the low mobility of transceivers of wireless backhaul channels, this setup ensures that the delay over each single hop is lower than the coherence time of LoS channels in the centimeter wave range [13], [14], which is commonly used for such channels. Among all the parameters, there are four that are of particular interest to us to test the sensitivity of our approach, namely the total time frame length T_{\max} , the number of hops I , the decoding/feedback delay T_1 , and the mean channel gain $\bar{\gamma}$. Each of these key parameters is assigned with a default value and a test range. When benchmarking the approaches regarding one key parameter over its test range, all the rest key parameters are specified to their default values. For every individual specification, $n_{\text{MC}} = 1\,000\,000$ runs of Monte-Carlo test are conducted, each run with an independently generated set of channel conditions for the I hops, with which all approaches are tested.

C. Results and Analyses

The results of sensitivity tests regarding T_{\max} , I , T_1 and $\bar{\gamma}$ are illustrated in Fig. 4. Generally, the E2E packet loss rate monotone increase as *i*) the average blocklength that can be allocated to each hop (exclusive the decoding/feedback delay) decreases; and *ii*) the SNR decreases.

We observe from the results that the DMH-HARQ approach consistently outperforms all baselines, even when under an unfair disadvantage in soft combining. It is promised to hold even more performance gain over the static HARQ solutions when applied with a more advanced combining technology. This excellent performance is credited to the DP algorithm that guarantees to achieve the theoretical maximum of the Bellman sum (14). Especially, with more available blocklength per hop, since the overall possible numbers of HARQ attempts over the I -hop chain increases, this performance gain brought by DP is also increasing. To the contrary, when the channel is harsh or the radio resource is extremely limited, the constraint (6b) is likely forcing to allow only one transmission slot per hop, so that the optimal DMH-HARQ schedule converges to the optimal one-shot-per-hop schedule, which just gives the performance upper bound of optimal static HARQ-IR in

TABLE I: Setup of the simulation campaign

Parameter	Value	Remark
f_s	250kSPS	Symbol rate, corresponding to a 4 μ s symbol duration
Q_m	1	Modulation order, 1 for BPSK
P	1 mW	Transmission power
N	1 mW	Noise power
d	16 bit	Payload of each message
ε_{\max}	0.5	Maximal allowed PER per transmission
T_{\max}	1 ms	Default time frame length
\mathbf{T}_{\max}	{0.4, 0.5, ..., 1} ms	Test range of time frame length
I	4	Default number of hops
\mathbf{I}	{2, 3, ..., 10}	Test range of hops number
$L_{f,i}$	\sim Rice(0.5, 1)	Small-scale fading with a consistent line-of-sight (LoS) path
T_1	12 μ s	Default decoding/feedback delay
\mathbf{T}_1	{10, 20, ..., 100} μ s	Test range of decoding/feedback delay
\bar{g}	0 dB	Mean channel gain
$\mathbf{\bar{g}}$	{-10, -9, ..., 0} dB	Test range of mean channel gain
n_{MC}	1 000 000	Runs per Monte-Carlo test

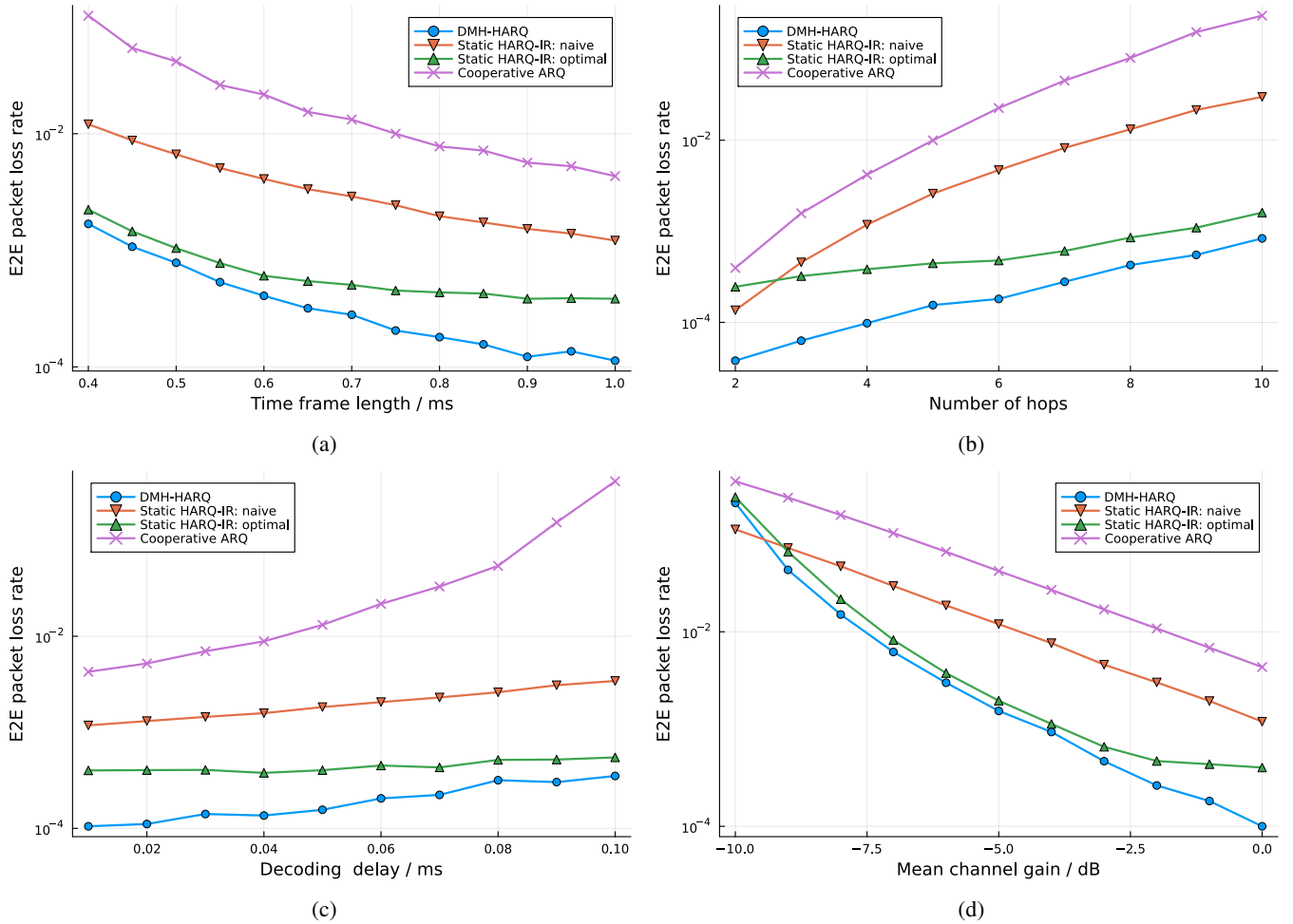


Fig. 4: Sensitivity tests regarding (a) the time frame length, (b) the number of hops, (c) the decoding/feedback delay, and (d) the pathloss, respectively.

FBL [5]. Moreover, the performance gain of DMH-HARQ over the baselines remains significant when the number of hops increases.

Remark that the listening-based cooperative ARQ approach also allocates the radio resource to different hops in a technically dynamic manner. However, its mechanism design only allows the successor hops to inherit unused resource from predecessors, not the other way around. With a same fixed blocklength for every (re)transmission, it results in a longer effective sub-frame for the late hops that are closer to the final information sink than the for early hops that are closer to the source. However, as it can be derived from [39], as a stochastic DP, the optimal solution shall be just the opposite: to allocate more resource to the early hops than the late ones. In the end, the listening-based cooperative ARQ approach cannot hit the optimum of the DP problem (6), and has only a limited gain from the dynamic scheduling. This impact is even more critical in the FBL regime where ARQ/HARQ generally work poor, leading to a significant gap to the performance in the infinite blocklength (IBL) regime. As we see from the results, the listening-based cooperative ARQ approach performs the worst among all baselines.

VII. FURTHER DISCUSSIONS

A. LUT Implementation: Complexity and Performance

As we have discussed in Sec. V-C, the requirement of real-time online solution suggests a LUT-based implementation of the DMH-HARQ method. As the price for the significant time complexity reduction from $\mathcal{O}(n_{\text{MAX}}^I)$ to $\mathcal{O}[\log((n_{\text{MAX}}))]$, extra space complexity must be taken into account. As we have already shown, for any given SNR γ , the allocation policy n_{opt} is a function of remaining time t and the number of remaining hops i . Thus, the size of the LUT implemented at each relaying node is (loosely) upper-bounded by $I_{\text{max}} n_{\text{MAX}} L$, where n_{MAX} is the maximum number of blocklength in a radio frame, and L is the number of discrete SNR levels. Here we carry out a worst-case analysis for a rough estimate of the memory cost to assess the deployment feasibility.

I_{max} , as aforementioned, is constrained by the E2E latency limit T_{max} , which is typically in the range of tens to hundreded milliseconds in our investigated use scenarios. Moreover, for every specific deployment, I is determined by the overall distance of wireless backhaul and the radio coverage of each relay node, which depends on the frequency band. For long-distance backhaul where rural environments are commonly considered, the traditional sub-40 GHz band is preferred and its typical link length (per hop) is around 15 km. For midhaul connections in suburban areas, this length reduces to 8 km per hop [40]. According to [38], relay chains in midhails can reach a distance of 40 km and in backhails up to 300 km, we can reasonably consider that $I_{\text{max}} \leq 25$ even in the utmost case. n_{MAX} , on the other hand, depends on the specific radio frame design for the wireless transport network, and is also constrained by the latency limit T_{max} . At last, the SNR quantization levels L can be flexibly configured. However, a small L implies higher CSI quantization error, which will certainly degrade the performance. To assess this effect and select

the proper L , we repeated the benchmark test with default specifications listed in Tab. I, but with L -level quantized CSI instead of accurate CSI at each node. The results are illustrated in Fig. 5, which suggests to pick $L \geq 64$, so that significant performance loss can be avoided to sufficiently leverage the performance gain of DMH-HARQ.

Given these parameter values, to provide a realistic estimate of the time and memory costs of the LUT implementation, we benchmarked the computation of $L = 64$ LUTs regarding Algorithm 1 under different scenarios. The system specifications and the benchmark results are listed in Tab. II, which shows that even for an extremely challenging scenario with $I_{\text{max}} = 25$, $n_{\text{MAX}} = 5000$, and $d = 128$, the offline LUT computation can be accomplished within 5.5 hours on a regular commercial workstation, and the total size of the generated LUTs is barely above 250 kB, which is negligible for modern communication devices.

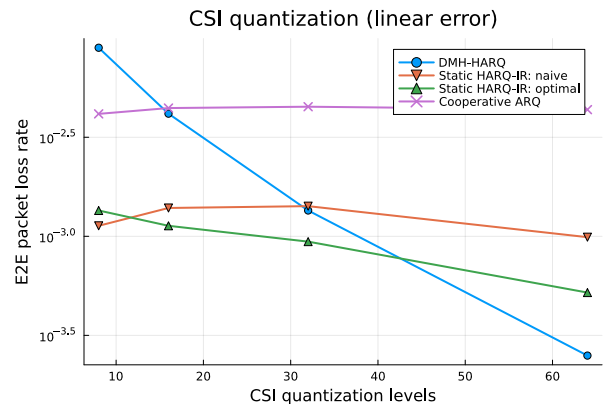


Fig. 5: Sensitivity test regarding the CSI quantization levels.

TABLE II: Cost of the offline LUT generation ($L = 64$)

Testing Platform	CPU	Memory
	AMD Ryzen 5 5600G @ 3.9 GHz 6 cores, 12 threads 64 bit, 7 nm process	32 GB DDR4-2133 MHz Dual-channel
	Operation System	LUT Solver
	Windows 11 Pro	Julia 1.11.6
Scenario	Time	Memory
$n_{\text{MAX}} = 100, I_{\text{max}} = 2, d = 16$	464.8 ms	4.876 kB
$n_{\text{MAX}} = 500, I_{\text{max}} = 4, d = 32$	31.21 s	27.62 kB
$n_{\text{MAX}} = 1000, I_{\text{max}} = 10, d = 64$	4.021 min	48.20 kB
$n_{\text{MAX}} = 5000, I_{\text{max}} = 25, d = 128$	5.467 h	250.88 kB

B. Imperfect CSI Measurement at Local Hop

While we have assumed that each node has perfect CSI at its local hop and statistical CSI at all hops thereafter, it shall be noted that in practical systems, even the CSI measurement at the local hop can be inaccurate or outdated, and some performance degradation will occur in this case, in addition to the impact of the CSI quantization error. Nevertheless, for wireless backhaul and midhaul scenarios where both the transmitter and receiver are mounted at high altitudes with stable positions, the channel variation is generally slow, and

the CSI can be accurately estimated with low overhead. Moreover, it is not only our proposed DMH-HARQ scheme that will be affected by such imperfect CSI. Conventional solutions, such like the static HARQ-IR, also rely on CSI to perform optimal blocklength allocation. It is therefore of generic interest to minimize the CSI estimation error and its impact on system performance, which is beyond the scope of this article.

C. Timer Overhead

While the DMH-HARQ approach requires a timer field embedded in the message header, it is also worth a discussion to assess its overhead. The timer field must contain sufficient bits to represent the remaining symbols in the current multi-hop forwarding session, so it is lower-bounded by $\lceil \log_2(n_{\text{MAX}}) \rceil$. We consider the same four scenarios as listed in Tab. II, and calculate the timer-to-payload bit length ratio for each, as shown in Tab. III. Generally, for small data packets over short relay chains, the overhead is significant but acceptable compared to the typical channel coding redundancy, considering the reliability gain it offers. Moreover, this overhead ratio further decreases in long-distance scenarios with larger packets, since the timer grows only logarithmically with n_{MAX} , while decreasing proportionally to the payload length.

TABLE III: Timer-to-payload length ratio of selected scenarios

Scenario	Min. Timer Bits	Ratio
$n_{\text{MAX}} = 100, d = 16$	4	25.00%
$n_{\text{MAX}} = 500, d = 32$	9	28.13%
$n_{\text{MAX}} = 1000, d = 64$	10	15.63%
$n_{\text{MAX}} = 5000, d = 128$	13	10.16%

D. Incremental Redundancy Gain

We have proven that even when applied without any combining technique, DMH-HARQ is able to outperform the optimal static HARQ-IR. A natural idea, of course, is to further enhance the performance of DMH-HARQ with soft combining, especially with an ideal IR, where the PER formula (9) must be replaced by

$$\varepsilon_s = Q \left(\sqrt{\frac{n_s + \frac{\tau_s}{T_b}}{V_{I+1-i_s}}} \left(C_{I+1-i_s} - \frac{d}{n_s + \frac{\tau_s}{T_b}} \right) \ln 2 \right). \quad (16)$$

Though IR is guaranteed to reduce the achievable E2E packet loss rate of DMH-HARQ, it costs more computational effort. The inclusion of τ_s into ε_s rejects Lemma 1. To keep it an MDP so that the integer DP based framework of Algorithm 1 still applies, τ_s must play its role as part of the system state when solving the decision policy, i.e. n_s . The dictionaries $\mathcal{D}_{\text{local}}$ and $\mathcal{D}_{\text{succ}}$ in Algorithm 1 shall map $[t_s, i_s, \tau_s]$ instead of $[t_s, i_s]$ to $[\xi_{\text{opt}}, n_{\text{opt}}]$. This will significantly increase the effective size of the state space, raising the time complexity of solving n_s at each node from $\mathcal{O}(n_{\text{MAX}}^I)$ to $\mathcal{O}(n_{\text{MAX}}^{2I})$.

E. Multi-Access Design

In this paper we have been focusing on a single multi-hop data link. In practical deployment, a multi-access solution will be mandatory to allow efficient networking, especially in the fronthaul and midhaul domains, where the network exhibits a star topology that each O-DU is associated with multiple O-RUs and each O-CU with multiple O-DUs. While OFDMA is widely used in modern radio systems and has been dominating most wireless standards, it may not be the optimal match for our DMH-HARQ protocol, due to the challenge in interference management caused by the dynamic traffic pattern that are hard to predict. Similar issue has already been discussed for the original CLARQ problem [36], revealing that time-division multiple access (TDMA) will be a better solution than OFDMA in this context. This will limit the application of the dynamic HARQ approaches such like CLARQ or DMH-HARQ for the air interface between users and base stations, which are generally standardized in modern cellular systems to use OFDMA for better scalability and flexibility. It is also for this reason that we exclude the air interface from the scope of this study.

However, in wireless transport networks which is under our focus in this study, TDMA can still be a good and feasible option, because: *i*) unlike the air interface of Radio Access Network (RAN), the physical layer design of transport network is not universally standardized but upon the design of vendor, allowing to use TDMA; *ii*) compared to the number of user equipments (UEs) in RAN, the number of transport network nodes are limited, leading to low demand for scalability; *iii*) the transport network nodes are generally installed at fixed position, leading to easy synchronization and low demand for flexibility.

Moreover, the TDMA design in DMH-HARQ can be potentially combined with the target wake time (TWT) mechanism, which is utilized by the IEEE 802.11ax standard, to further raise the time efficiency of DMH-HARQ: after successfully forwarding a message, the relaying node can send a triggering token to the next transmitting node, so that it is immediately waken from sleep and start its the DMH-HARQ process, instead of waiting till the last transmitting node completing its multi-hop relay. In such way, multiple data links can be parallelized in a pipeline fashion over the multiple hops, so that the E2E delay is reduced.

VIII. CONCLUSION AND OUTLOOKS

In this paper, we have looked into the problem of dynamic HARQ in multi-hop wireless transport network with a special focus on reliability and openness. Considering FBL regime, we have proposed a DMH-HARQ scheme with an associated DP algorithm that optimizes it. The proposed methods are proven via numerical simulations as effective and outperforming conventional baselines, even without any code combining. Its performance superiority remains consistent regarding the link delay budget and decoding delay, and increases along with the hop number and the channel quality.

As for the next step, we plan to apply IR to DMH-HARQ, and extend our analyses and optimization methods in this

paper thereto. Deeper study to the multiple access design for DMH-HARQ and its integration with TWT mechanism is also an interesting topic for future study.

ACKNOWLEDGMENT

This work is partially supported by the German Federal Ministry of Education and Research in the programme of ‘‘Souverän. Digital. Vernetzt.’’ joint projects 6G-RIC (16KISK028) and Open6GHub (16KISK003K/16KISK004/16KISK012). This work is partially supported by SNS JU Project 6G-GOALS (GA no. 101139232).

APPENDIX A

PROOF OF LEMMA 2

Proof. For the last hop ($i_s = 1$), consider an *arbitrary* DMH-HARQ scheme with maximal K transmission attempts, where the blocklength of k^{th} (re-)transmission is m_k for all $k \in \{1, 2, \dots, K\}$. Obviously, since $i_s = 1$, the utility equals the overall chance of successful transmission. Using Type I HARQ without combining, that is

$$\begin{aligned} \xi &= 1 - \epsilon_I(m_1) + \epsilon_I(m_1) [1 - \epsilon_I(m_2)] \\ &\quad + \epsilon_I(m_1)\epsilon_I(m_2) [1 - \epsilon_I(m_3)] + \dots \\ &\quad + \epsilon_I(m_1) \dots \epsilon_I(m_{K-1}) [1 - \epsilon_I(m_K)] \\ &= 1 - \prod_{k=1}^K \epsilon_I(m_k) \end{aligned} \quad (17)$$

Meanwhile, according to [5], if it is Type-II HARQ with IR applied, the overall chance of successful transmission is equivalent to that of an *one shot* transmission:

$$\xi_{\text{os}} = 1 - \epsilon_I \left(\sum_{k=1}^K m_k \right). \quad (18)$$

Obviously, under the same blocklength allocation and channel conditions, Type II HARQ-IR always outperforms Type I HARQ without combining in error rate, i.e., $\prod_{k=1}^K \epsilon_I(m_k) \geq \epsilon_I \left(\sum_{k=1}^K m_k \right)$, which takes the equality only when $K = 1$. Furthermore, given the fixed remaining time t_s , we always have the constraint $\sum_{k=1}^K (m_k T_b + T_1) \leq t_s$, which means

$$\sum_{k=1}^K m_k \leq \frac{t_s - K T_1}{T_b} \leq \frac{t_s - T_1}{T_b}, \quad (19)$$

where the first equality is taken only when t_s is sufficiently exploited, and the second taken only when $K = 1$. Additionally, it always holds that $\partial \epsilon_I(m) / \partial m < 0$ for all $m \in \mathbb{R}^+$. Thus, we have

$$\prod_{k=1}^K \epsilon_I(m) \geq \epsilon_I \left(\frac{t_s - T_1}{T_b} \right), \quad (20)$$

where the equality is only taken when $K = 1$ and $m_1 = \frac{t_s - T_1}{T_b}$, and the Lemma is therewith proven. \square

APPENDIX B PROOF OF THEOREM 1

Proof. For the first step, we prove the monotone of $\xi_{\max}(s)$ regarding t_s as follows. Given any feasible system status $s_0 = (t_{s_0}, i_{s_0}, k_{s_0}, \tau_{s_0})$, let n_{opt} be an optimal blocklength allocation policy¹ that generates the DMH-HARQ schedule $\mathfrak{T}_{s_0}^{\text{opt}}$ with maximized utility $\xi_{\max}(s_0)$. According to Lemma 2, there must be $n_{\text{opt}}(s) = \frac{t_s}{T_b} - T_1$ for all s that $i_s = 1$.

Given an *arbitrary* $\Delta t > 0$, let $s^{<\Delta t>}$ denote $(t_s + \Delta t, i_s, k_s, \tau_s)$, we can always construct a sub-optimal n_{sub} that

$$n_{\text{sub}}(s) = \begin{cases} n_{\text{opt}}(s^{<-\Delta t>}) + \frac{\Delta t}{T_b} & i_s = 1, \\ n_{\text{opt}}(s^{<-\Delta t>}) & \text{otherwise.} \end{cases} \quad (21)$$

Now apply n_{sub} on the initial state $s_1 = s_0^{\Delta t}$ to generate another DMH-HARQ schedule $\mathfrak{T}_{s_1}^{\text{sub}}$, it is straightforward to derive that $\mathfrak{T}_{s_0}^{\text{opt}}$ and $\mathfrak{T}_{s_1}^{\text{opt}}$ have the identical structure, except that for each non-empty node s in $\mathfrak{T}_{s_0}^{\text{opt}}$, the corresponding node of $\mathfrak{T}_{s_1}^{\text{opt}}$ is

$$s' = \begin{cases} s & i_{s'} = 0, \\ s^{<\Delta t>} & \text{otherwise.} \end{cases} \quad (22)$$

And error rates of each transmission attempt regarding the two schedules, denoted as ϵ_s and $\epsilon_{s'}$, respectively, must fulfill

$$\epsilon_{s'} = \begin{cases} < \epsilon_s & i_{s'} = 1, \\ \epsilon_s & \text{otherwise.} \end{cases} \quad (23)$$

Recalling Eq. (14), it always hold $\xi(\mathfrak{T}_{s_1}^{\text{sub}}) > \xi_{\max}(s_0)$. Meanwhile, there is always some n'_{opt} that generates an optimal schedule $\mathfrak{T}_{s_1}^{\text{opt}}$ with maximal $\xi_{\max}(s_1) \geq \xi(\mathfrak{T}_{s_1}^{\text{sub}})$. Thus:

$$\xi_{\max}(s_1) = \xi_{\max}(s_0^{<\Delta t>}) > \xi_{\max}(s_0) \quad \forall s_0, \forall \Delta t > 0, \quad (24)$$

i.e. $\xi_{\max}(s)$ is strictly monotone increasing regarding t_s .

Next, we come to prove the continuity of this function. According to Eq. (9), ϵ_s is continuous function of t_s , so $\xi_{\max}(s)$ can be guaranteed t_s -continuous, if both $\xi_{\max}(s_1(\mathfrak{T}_s))$ and $\xi_{\max}(s_r(\mathfrak{T}_s))$ are continuous functions of t_s . This sufficient condition can be derived via mathematical induction as follows.

Starting with the two *termination cases* of $t_s < T_{\min}^{(i_s)}$ and $i_s = 0$, respectively, according to Eqs. (1) and (2) we have $S(L(\mathfrak{T}_s)) = S(R(\mathfrak{T}_s)) = \emptyset$. Recalling (5), for the termination cases we have $\xi_{\max}(s) = \xi(\mathfrak{T}_s) \equiv 0$, which are both t_s -continuous. Therefore, the utility $\xi_{\max}(s)$ itself is also t_s -continuous.

Then consider the last hop where $i_s = 1$, according to Lemma 2 we know that $\xi_{\max}(s)$ is achieved when $n_s = \frac{t_s - T_1}{T_b}$, leading to a left branch where $t_{s_1}(\mathfrak{T}_s) = 0 < T_{\min}^{(1)}$ and a right branch where $i_{s_r}(\mathfrak{T}_s) = 0$, both are termination cases. Thus, as proven above we have both $\xi_{\max}(s_1(\mathfrak{T}_s))$ and $\xi_{\max}(s_r(\mathfrak{T}_s))$ are t_s -continuous, and therefore $\xi_{\max}(s)$ the same as well.

For other hops other than the last one, i.e. $i_s \in \{2, 3, \dots, I\}$, according to the DMH-HARQ principle (1) and (2), it is

¹The existence of such optima is guaranteed by the bounded range of $\xi(s_0)$. However, the uniqueness of n_{opt} is not guaranteed. Hence we use the term ‘‘an optimal policy’’ instead of ‘‘the optimal policy’’ here.

obvious that there are only three possible combinations of its left and right branches:

- 1) $s_1(\mathfrak{T}(s)) = \emptyset, i_{s_r}(\mathfrak{T}(s)) = \emptyset;$
- 2) $s_1(\mathfrak{T}(s)) = \emptyset, i_{s_r}(\mathfrak{T}(s)) = i_s - 1;$
- 3) $i_{s_1}(\mathfrak{T}(s)) = i_s, i_{s_r}(\mathfrak{T}(s)) = i_s - 1.$

For case 1), $\xi_{\max}(s) \equiv 0$, which is t_s -continuous. For case 2), $\xi_{\max}(s_1(\mathfrak{T}(s)))$ is t_s -continuous as proven above, so that $\xi_{\max}(s)$ can be guaranteed t_s -continuous if only $\xi_{\max}(s_r(\mathfrak{T}(s)))$ is t_s -continuous. For case 3), we recall Lemma 1 that $n_{\text{opt}}(s)$ depends only on t_s and i_s , so that $\xi_{\max}(\mathfrak{T}(s))$ and $\xi_{\max}(L(\mathfrak{T}(s)))$ are different samples for the *same* function of t_s . Since the iterative generation of the left branch in decision tree is determined to terminate with an empty set, i.e. case 1) or 2), we can conclude that for a \mathfrak{T}_s in case 3), both $\xi_{\max}(s)$ and $\xi_{\max}(s_1(\mathfrak{T}(s)))$ are guaranteed t_s -continuous if $\xi_{\max}(s_r(\mathfrak{T}(s)))$ is t_s -continuous. Since the iterative generation of the right branch in decision tree always ends up with one of the two termination cases, which are both t_s -continuous, we can conclude from the analyses above that $\xi_{\max}(s)$ is also t_s -continuous for all s where $i_s > 1$.

Thus, the continuity is proven for all $i \in \mathcal{S}$. With both the monotone and the continuity derived, the theorem is proven. \square

REFERENCES

- [1] N. Athanasopoulos, P. Tsiakas, K. Voudouris, I. Georgas, and G. Agapiou, "Multi-hop relay in next generation wireless broadband access networks: An overview," in *International Conference on Mobile Lightweight Wireless Systems*. Springer, pp. 543–554, 2010.
- [2] S. Karmakar and M. K. Varanasi, "The diversity-multiplexing tradeoff of the dynamic decode-and-forward protocol on a MIMO half-duplex relay channel," *IEEE Transactions on Information Theory*, vol. 57, no. 10, pp. 6569–6590, 2011.
- [3] O. Adamuz, V. Sciancalepore, P. Ameigeiras, J. M. Lopez-Soler and X. Costa-Perez, "A Stochastic Network Calculus (SNC)-Based Model for Planning B5G uRLLC RAN Slices," *IEEE Transactions on Wireless Communications*, vol. 22, no. 2, pp. 1250–1265, 2022.
- [4] Y. Hu, J. Gross, and A. Schmeink, "On the capacity of relaying with finite blocklength," *IEEE Transactions on Vehicular Technology*, vol. 65, no. 3, pp. 1790–1794, 2016.
- [5] B. Makki, T. Svensson, and M. Zorzi, "Finite block-length analysis of the incremental redundancy HARQ," *IEEE Wireless Communications Letters*, vol. 3, no. 5, pp. 529–532, 2014.
- [6] Samsung, "Virtualized radio access network: Architecture, key technologies and benefits." Technical Report, 2019.
- [7] A. Garcia-Saavedra and X. Costa-Pérez, "O-RAN: Disrupting the virtualized RAN ecosystem," *IEEE Communications Standards Magazine*, vol. 5, no. 4, pp. 96–103, 2021.
- [8] G. Garcia-Aviles, A. Garcia-Saavedra, M. Gramaglia, X. Costa-Perez, P. Serrano, and A. Banchs, "Nuberu: Reliable RAN virtualization in shared platforms," in *Proceedings of the 27th Annual International Conference on Mobile Computing and Networking*, ser. MobiCom '21. New York, NY, USA: Association for Computing Machinery, pp. 749–761, 2021.
- [9] B. Tezergil and E. Onur, "Wireless backhaul in 5G and beyond: Issues, challenges and opportunities," *IEEE Communications Surveys & Tutorials*, vol. 24, no. 4, pp. 2579–2632, 2022.
- [10] M. Jiang, J. Cezanne, A. Sampath, O. Shental, Q. Wu, O. Koymen, A. Bedewy, and J. Li, "Wireless fronthaul for 5G and future radio access networks: Challenges and enabling technologies," *IEEE Wireless Communications*, vol. 29, no. 2, pp. 108–114, 2022.
- [11] W. Jiang, B. Han, M. A. Habibi, and H. D. Schotten, "The road towards 6G: A comprehensive survey," *IEEE Open Journal of the Communications Society*, vol. 2, pp. 334–366, 2021.
- [12] J. Goel and H. Jagadeesh, "Listen to others' failures: Cooperative ARQ schemes for low-latency communication over multi-hop networks," *IEEE Transactions on Wireless Communications*, vol. 20, no. 9, pp. 6049–6063, 2021.
- [13] A. M. O. Ribeiro, E. M. M. Barrientos, and E. Conforti, "Spatial correlation function and coherence time characterization of 3.5-GHz micro-cell propagation," *2009 SBMO/IEEE MTT-S International Microwave and Optoelectronics Conference (IMOC)*, Belem, Brazil, pp. 501–505, 2009.
- [14] Y. Lu, M. Koivisto, J. Talvitie, M. Valkama, and E. S. Lohan, "Positioning-aided 3D beamforming for enhanced communications in mmWave mobile networks," *IEEE Access*, vol. 8, pp. 55513–55525, 2020.
- [15] O-RAN Alliance, "Working Group 7; Outdoor Micro Cell Hardware Architecture and Requirements (FR1) Specification; V01.00," Alfter, Germany, Jun. 2021.
- [16] M. Mohsin, J. M. Batalla, E. Pallis, G. Matorakis, E. K. Markakis, and C. X. Mavromoustakis, "On analyzing beamforming implementation in O-RAN 5G," *Electronics*, vol. 10, no. 17, 2021.
- [17] A. Chaaban and A. Sezgin, "Multi-hop relaying: An end-to-end delay analysis," *IEEE Transactions on Wireless Communications*, vol. 15, no. 4, pp. 2552–2561, 2016.
- [18] K. Dhaka, R. K. Mallik, and R. Schober, "Performance analysis of decode-and-forward multi-hop communication: A difference equation approach," *IEEE Transactions on Communications*, vol. 60, no. 2, pp. 339–345, 2012.
- [19] G. Farhadi and N. C. Beaulieu, "Fixed relaying versus selective relaying in multi-hop diversity transmission systems," *IEEE Transactions on Communications*, vol. 58, no. 3, pp. 956–965, 2010.
- [20] J. Ibrahim, A. Rehman, M. S. B. Ilyas, M. Shehzad, and M. Ashraf, "Optimization and traffic management in IEEE 802.16 multi-hop relay stations using genetic and priority algorithms," *International Journal of Computer Science and Information Security*, vol. 14, no. 7, p. 599, 2016.
- [21] S. Maagh, M. Y. Sharif, and A. Almaini, "On the dynamic decode-and-forward relay listen-transmit decision rule in intersymbol interference channels," in *Proceedings of the 9th WSEAS International Conference on Data Networks, Communications, Computers*, pp. 26–29, 2010.
- [22] M. A. Habibi, F. Z. Yousef, and H. D. Schotten, "Mapping the VNFs and VLS of a RAN slice onto intelligent PoPs in beyond 5G mobile networks," *IEEE Open Journal of the Communications Society*, vol. 3, pp. 670–704, 2022.
- [23] C. C. Zhang, K. K. Nguyen, and M. Cheriet, "Joint routing and packet scheduling for URLLC and eMBB traffic in 5G O-RAN," in *ICC 2022 - IEEE International Conference on Communications*, pp. 1900–1905, 2022.
- [24] Y. Polyanskiy, H. V. Poor, and S. Verdú, "Channel coding rate in the finite blocklength regime," *IEEE Transactions on Information Theory*, vol. 56, no. 5, pp. 2307–2359, 2010.
- [25] Y. Polyanskiy, H. V. Poor, and S. Verdú, "Dispersion of the Gilbert-Elliott channel," in *2009 IEEE International Symposium on Information Theory*, pp. 2209–2213, 2009.
- [26] W. Yang, G. Durisi, T. Koch, and Y. Polyanskiy, "Quasi-static multiple-antenna fading channels at finite blocklength," *IEEE Transactions on Information Theory*, vol. 60, no. 7, pp. 4232–4265, 2014.
- [27] M. Effros, V. Kostina, and R. C. Yavas, "Random access channel coding in the finite blocklength regime," in *2018 IEEE International Symposium on Information Theory (ISIT)*, pp. 1261–1265, 2018.
- [28] X. Zhang, J. Wang, and H. V. Poor, "Statistical delay and error-rate bounded QoS provisioning for mURLLC over 6G CF M-MIMO mobile networks in the finite blocklength regime," *IEEE Journal on Selected Areas in Communications*, vol. 39, no. 3, pp. 652–667, 2021.
- [29] B. Han, Y. Zhu, Z. Jiang, M. Sun, and H. D. Schotten, "Fairness for freshness: Optimal age of information based OFDMA scheduling with minimal knowledge," *IEEE Transactions on Wireless Communications*, vol. 20, no. 12, pp. 7903–7919, 2021.
- [30] X. Sun, S. Yan, N. Yang, Z. Ding, C. Shen, and Z. Zhong, "Short-packet downlink transmission with non-orthogonal multiple access," *IEEE Trans. Wireless Commun.*, vol. 17, no. 7, pp. 4550–4564, 2018.
- [31] Y. Zhu, Y. Hu, A. Schmeink, and J. Gross, "Energy minimization of mobile edge computing networks with HARQ in the finite blocklength regime," *IEEE Transactions on Wireless Communications*, vol. 21, no. 9, pp. 7105–7120, 2022.
- [32] Y. Hu, A. Schmeink, and J. Gross, "Optimal scheduling of reliability-constrained relaying system under outdated CSI in the finite blocklength regime," *IEEE Transactions on Vehicular Technology*, vol. 67, no. 7, pp. 6146–6155, 2018.
- [33] C. Pan, H. Ren, Y. Deng, M. El-kashlan, and A. Nallanathan, "Joint blocklength and location optimization for URLLC-enabled UAV relay systems," *IEEE Communications Letters*, vol. 23, no. 3, pp. 498–501, 2019.

- [34] Y. Hu, Y. Zhu, M. C. Gursoy, and A. Schmeink, "SWIPT-enabled relaying in IoT networks operating with finite blocklength codes," *IEEE Journal on Selected Areas in Communications*, vol. 37, no. 1, pp. 74–88, 2019.
- [35] A. Agarwal, A. K. Jagannatham, and L. Hanzo, "Finite blocklength non-orthogonal cooperative communication relying on SWIPT-enabled energy harvesting relays," *IEEE Transactions on Communications*, vol. 68, no. 6, pp. 3326–3341, 2020.
- [36] B. Han, Y. Zhu, M. Sun, V. Sciancalepore, Y. Hu, and H. D. Schotten, "CLARQ: A dynamic ARQ solution for ultra-high closed-loop reliability," *IEEE Transactions on Wireless Communications*, vol. 21, no. 1, pp. 280–294, 2022.
- [37] B. Han, Y. Zhu, A. Schmeink, and H. D. Schotten, "Time-energy-constrained closed-loop FBL communication for dependable MEC," in *2021 IEEE Conference on Standards for Communications and Networking (CSCN)*, pp. 180–185, 2021.
- [38] J. Gomes, J. A. L. Silva, and M. E. V. Segatto, "Reducing the 5G fronthaul traffic with O-RAN," in *2019 SBMO/IEEE MTT-S International Microwave and Optoelectronics Conference (IMOC)*, pp. 1–3, 2019.
- [39] R. Bellman, "Some problems in the theory of dynamic programming," *Econometrica: Journal of the Econometric Society*, pp. 37–48, 1954.
- [40] C. Han, J. Huo, Q. Gao, G. Su, and H. Wang, "Rainfall monitoring based on next-generation millimeter-wave backhaul technologies in a dense urban environment," *Remote Sensing*, vol. 12, no. 6, p. 1045, 2020.



Bin Han (Senior Member, IEEE) received his B.E. degree in 2009 from Shanghai Jiao Tong University, M.Sc. in 2012 from the Technical University of Darmstadt, and a Ph.D. degree in 2016 from Karlsruhe Institute of Technology. He joined University of Kaiserslautern-Landau (RPTU) in 2016, and was granted his Habilitation (Venia Legendi) in 2023. His research interests are in the broad areas of wireless communications, mobile networks, and signal processing. He is the author of two books, six book chapters, and over 80 research papers. He has participated in multiple EU FP7, Horizon 2020, and Horizon Europe research projects. Dr. Han is Editorial Board Member for *Network* and Guest Editor for *Electronics*. He has served in organizing committee and/or TPC for *IEEE GLOBECOM*, *IEEE ICC*, *EuCNC*, *European Wireless*, and *ITC*. He is a Voting Member of the IEEE Standards Association Working Groups P1955, P2303, P3106, and P3454.



Muxia Sun (Member, IEEE) received in 2010 his B.Sc. degree from South China University of Technology (SCUT), M.Sc. in 2012 & 2013 from Université de Nantes and SCUT, respectively, and the Ph.D. degree in 2019 from Université Paris-Saclay. Since 2020 he has been with Tsinghua University as Postdoctoral Researcher in the Department of Industrial Engineering. His current research interests include reliability assessment and optimization of industrial & communication systems, robust optimization, and approximation algorithm design.



as well as physical layer security.

Yao Zhu (Member, IEEE) received the B.S. degree in electrical engineering from the University of Bremen, Bremen, Germany, in 2015, his master's degree and his Ph.D degree in electrical engineering, information technology and computer engineering from RWTH Aachen University, Aachen, Germany, in 2018 and 2022, respectively. He is currently a postdoctoral researcher with the Chair of Information Theory and Data Analytics. His research interests include ultra-reliable and low-latency communications, integrated sensing and communication,



best Ph.D. thesis in the area of communication technologies (Wireless and Networking) issued by GTTI in 2015. He is an Editor of *IEEE Transactions on Wireless Communications* and Editor of *IEEE Transactions on Communications*.

Vincenzo Sciancalepore (Senior Member, IEEE) received his M.Sc. degree in Telecommunications Engineering and Telematics Engineering in 2011 and 2012, respectively, whereas in 2015, he received a double Ph.D. degree. Currently, he is a senior 5G researcher at NEC Laboratories Europe GmbH in Heidelberg, focusing his activity on Smart Surfaces and Reconfigurable Intelligent Surfaces (RIS). He is currently involved in the IEEE Emerging Technologies Committee leading the initiatives on RIS. He was also the recipient of the national award for the



From 2011 to 2014, he worked as a radio access network engineer for HUAWEI. His main research interests include network slicing, network function virtualization, resource allocation, machine learning, and radio access network architecture.

Mohammad Asif Habibi received his B.Sc. degree in Telecommunications Engineering from Kabul University, Afghanistan, in 2011. He obtained his M.Sc. degree in Systems Engineering and Informatics from the Czech University of Life Sciences, Czech Republic, in 2016. Since January 2017, he has been working as a research fellow and Ph.D. candidate at the Division of Wireless Communications and Radio Positioning, Rheinland-Pfälzische Technische Universität Kaiserslautern-Landau (previously known as Technische Universität Kaisers-



ISEK research Area, RWTH Aachen University. His research interests are in information theory, optimal design of wireless communication systems. He has been invited to contribute submissions to multiple conferences. He was a recipient of the IFIP/IEEE Wireless Days Student Travel Awards in 2012. He received the Best Paper Awards at *IEEE ISWCS 2017* and *IEEE PIMRC 2017*, respectively. He served as a TPC member for many conferences. He was the lead editor of the URLLC-LoPIoT special issue in *Physical Communication*, and the organizer and chair of two special sessions in *IEEE ISWCS 2018* and *ISWCS 2020*. He is currently serving as an editor for *Physical Communication* (Elsevier), *EURASIP Journal on Wireless Communications and Networking*, and *Frontiers in Communications and Networks*.

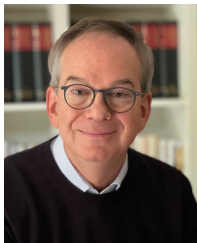
Yulin Hu (Senior Member, IEEE) received his M.Sc.E.E. degree from USTC, China, in 2011. In Dec. 2015 he received his Ph.D.E.E. degree (Hons.) from RWTH Aachen University where he was a postdoctoral Research Fellow since Jan. to Dec. in 2016. He was a senior researcher and team leader in ISEK research Area at RWTH Aachen University. From May to July in 2017, he was a visiting scholar in Syracuse University, USA. He is currently a professor with School of Electronic Information, Wuhan University, and an adjunct professor with



Anke Schmeink (IEEE Senior Member, Editor *IEEE Trans. Wireless Commun.*, Prof. Dr.-Ing.) is leading the Chair of Information Theory and Data Analytics at RWTH Aachen University, Germany. She received the Diploma degree in mathematics with a minor in medicine and the Ph.D. degree in electrical engineering and information technology from RWTH Aachen University, Germany, in 2002 and 2006, respectively. She worked as a research scientist for Philips Research before joining RWTH Aachen University. She spent several research visits with the University of Melbourne, and with the University of York. She is co-author of more than 270 publications and editor of the books *Big Data Analytics for Cyber-Physical Systems: Machine Learning for the Internet of Things* and *Smart Transportation: AI Enabled Mobility and Autonomous Driving*. Her research interests are in information theory, machine learning, data analytics and optimization with focus on wireless communications and medical applications.



Yan-Fu Li (Senior Member, IEEE) was a Faculty Member with the Laboratory of Industrial Engineering, CentraleSupélec, University of Paris-Saclay, Gif-sur-Yvette, France, from 2011 to 2016. He is currently a Professor with the Industrial Engineering Department, Tsinghua University, Beijing, China. He has led/participated in several projects supported by the European Union (EU), France, and Chinese Governmental funding agencies and various industrial partners. He has coauthored or coauthored more than 100 publications on international journals, conference proceedings, and books. His current research interests include reliability, availability, maintainability, and safety (RAMS) assessment and optimization with the applications onto various industrial systems. Dr. Li is an Associate Editor of *IEEE Transactions on Reliability*.



Hans D. Schotten (Member, IEEE) received the Ph.D. degree from the RWTH Aachen University, Germany, in 1997. From 1999 to 2003, he worked for Ericsson. From 2003 to 2007, he worked for Qualcomm. He became manager of a R&D group, Research Coordinator for Qualcomm Europe, and Director for Technical Standards. In 2007, he accepted the offer to become a Full Professor at Technische Universität Kaiserslautern. In 2012, he - in addition - became the Scientific Director of the German Research Center for Artificial Intelligence (DFKI) and Head of Department for Intelligent Networks. Professor Schotten served as Dean of Department of Electrical and Computing Engineering at Technische Universität Kaiserslautern from 2013 until 2017. Since 2018, he is the Chair of the German Society for Information Technology and a member of the Supervisory Board of the VDE. He has authored more than 200 papers and participated in over 30 European and national collaborative research projects.